Nanoscale Res Lett (2008) 3:321–329
DOI 10.1007/s11671-008-9160-2

NANO EXPRESS

Comparison of In vitro Nanoparticles Uptake in Various Cell Lines and In vivo Pulmonary Cellular Transport in Intratracheally Dosed Rat Model

Yurong Lai · Po-Chang Chiang · Jason D. Blom · Na Li · Kimberly Shevlin · Timothy G. Brayman · Yiding Hu · Jon G. Selbo · Liangbiao George Hu

Received: 7 July 2008 / Accepted: 18 August 2008 / Published online: 9 September 2008

Abstract In present study, the potential drug delivery of nanoformulations was validated via the comparison of cellular uptake of nanoparticles in various cell lines and in vivo pulmonary cellular uptake in intratracheally (IT) dosed rat model. Nanoparticles were prepared by a bench scale wet milling device and incubated with a series of cell lines, including Caco-2, RAW, MDCK and MDCK transfected MDR1 cells. IT dosed rats were examined for the pulmonary cellular uptake of nanoparticles. The processes of nanoparticle preparation did not alter the crystalline state of the material. The uptake of nanoparticles was observed most extensively in RAW cells and the least in Caco-2 cells. Efflux transporter P-gp did not prevent cell from nanoparticles uptake. The cellular uptake of nanoparticles was also confirmed in bronchoalveolar lavage (BAL) fluid cells and in bronchiolar epithelial cells, type II alveolar epithelial cells in the intratracheally administrated rats. The nanoparticles uptake in MDCK, RAW cells and in vivo lung epithelial cells indicated the potential applications of nanoformulation for poorly soluble compounds. The observed limited direct uptake of nanoparticles in Caco-2 cells suggests that the improvement in oral bioavailability by particle size reduction is via increased dissolution rate rather than direct uptake.

Keywords Cellular uptake · Nanoparticles · Intratracheally dosed rat model · P-glycoprotein

Abbreviations

MDCK	Madin-Darby canine kidney epithelial cell
RAW cell	The murine macrophage-like cell lines
Caco-2	Human colon adenocarcinoma cell
BAL	Bronchoalveolar lavage

Y. Lai (✉)
Pharmacokinetic, Dynamics, & Metabolism, Pfizer, Inc. St. Louis Laboratory, 700 Chesterfield Parkway West, Chesterfield, MO 63017, USA
e-mail: yurong.lai@pfizer.com

Y. Lai · P.-C. Chiang · J. D. Blom · N. Li · K. Shevlin · T. G. Brayman · Y. Hu · J. G. Selbo · L. G. Hu
Pfizer Global Research & Development, St. Louis Laboratories, Pfizer Inc, St. Louis, MO 63017, USA

P.-C. Chiang (✉)
Pharmaceutical Science, Pfizer, Inc. St. Louis Laboratory, Chesterfield, USA
e-mail: po-chang.chiang@pfizer.com

L. G. Hu (✉)
Drug Safety Research Development, Pfizer, Inc. St. Louis Laboratory, Chesterfield, USA
e-mail: george.hu@pfizer.com

Introduction

In association with slow dissolution characteristics, poor permeability and/or the involvement of efflux transporters, poorly aqueous soluble/permeable drugs present a challenging problem for drug formulation development due to the limitation of drug absorption in the gastrointestinal (GI) tract. In an environment of ever increasing drug entities with these characteristics where conventional formulation techniques are not efficient to develop poorly water-soluble compounds into drug products [1], novel approaches to overcome these factors are of great importance. Among the various solubility/dissolution rate enhancement methodologies available, particle size reduction is most commonly employed by formulators to improve bioavailability. Particle size reduction leads to increased dissolution and

solubility characteristics and offers improvement in bioavailability as outlined by the Ostwald-Feundlich equations [2]. In addition, size reduction to the nanometer range of 10–1000 nm, termed nanoparticles [3], has been shown to greatly improve exposure [4]. An outstanding feature of nanoparticles is the greater surface area consequently resulting in the increase in saturation solubility and the increase in dissolution rate of the compounds. Recently, nanoparticles have been reported to cross the intestinal epithelial barrier or rapidly diffuse from the lungs into the systemic circulation [5, 6]; however, the route, mechanism and extents to which this occurs are not yet entirely clear.

The pharmaceutical industry has invested heavily in the area of non-invasive delivery systems for GI poorly absorbed or unstable molecules. One of the most important aspects of systemic or local drug delivery routes has been targeting drug delivery into the lungs. Accordingly, techniques and new drug delivery devices intended to deliver drugs into the lungs have been widely developed in the last few years. Cellular uptake studies have demonstrated that besides macrophages, other cell lines like cancer cells and epithelial cells are also able to take up nanoparticles [7–9]. A hypothesis, which has not been widely investigated so far, is that the variations of nanoparticles uptake in vivo are observed in different tissue or cell barriers. To elucidate the hypothesis, in this study, we investigated the uptakes and transport of water-insoluble nanoparticles in various cell lines and in a nanoparticle IT injected rat model.

Materials and Methods

Nanoparticle Formulation

For particle size reduction, a bench scale wet milling (micronization) device was used [10]. To make the stock nanosuspension formulation (20 mg/mL) pyrene (GC grade from Fluka Chemical, Switzerland) or charcoal (acid washed with hydrochloric acid, cell culture tested, Sigma-Aldrich), an appropriate amount of glass beads, and 0.1% (w/w) Tween 80 in phosphate buffered saline (pH 7.4) were added in a scintillation vial. The mixture was then stirred at 1200 rpm for a period of 48 h with occasional shaking. The stock formulation was harvested and the potency of suspension and supernatant were examined by HPLC/UV.

Evaluation of Solid State Properties

Powder X-ray diffraction (PXRD) was used to confirm the solid state properties pre- and post-milling of pyrene, and conducted with a Bruker D-8 Advance diffractometer. The system used a copper X-ray source maintained at 40 kV and 40 mA to provide radiation with intensity weighted average of 1.54184 Å ($K\alpha_{ave}$). A scintillation counter was used for detection. Data were collected using a step scan of 0.02° per point with a 1 s/point counting time over a range of 3°–35° two-theta. In-house fabricated aluminum inserts or inserts with a Hasteloy sintered filter (0.45 μm) pressed in the center and held in Bruker plastic sample cup holders were utilized for all analyses. Dry pyrene was run as received without hand grinding. Suspensions were filtered onto sintered filters under vacuum. Particle size distribution was determined on a Beckman Coulter LS 230 particle size analyzer using a small volume accessory. Distributions from 2000 μm to 0.04 μm were generated using Mie scattering theory and a polarization intensity differential scattering obscuration optical model (PIDS) with sample obscurations held between 45% and 55%. There was no absorption by pyrene at the scattering wavelengths so the average index of refraction was determined by optical microscopy using index matching fluids (Cargille catalog #18005).

Cell Culture

Caco-2 cells (Pfizer Global batch) were maintained in Dulbecco's Modified Eagle's Medium (DMEM) supplemented with 10% fetal bovine serum, 1% non-essential amino acids, 1% Glutamax, 1 mM sodium pyruvate, and 0.06 mg/mL Gentamicin. MDCK and MDCK-MDR1 cells were cultured in minimum essential medium (MEM) with Earle's salts and L-glutamine containing 10% fetal bovine serum (FBS), 100 units penicillin, and 100 μg/mL streptomycin. The murine macrophage-like cells (RAW cells, ATCC TIB 71) were cultured in DMEM supplemented with 4 mM L-glutamine and 10% (v/v) FBS. All media and reagents were obtained from the Gibco BRL (Carlsbad, CA).

Cells were seeded at a density of 1×10^6 cells/mL in a glass chamber slide (Nalge Nunc International, NY) with regular changes in media. The uptake experiments were conducted after cell reaching confluence in a chamber slide. For nanoparticle uptake, the cells were washed with fresh medium and medium was replaced with nanoparticle suspension (0.05 mg/mL). The cells then were incubated at 37 °C in a humidified 5% CO_2/95% air atmosphere. At 2 and 4 h post-incubation, the glass slide chambers were completely washed with HBSS buffer to remove the non-specific binding particles. The cells were fixed with either 10% paraformaldehyde (for Pyrene nanoparticles) for 30 min or the fixative from the Diff-Quik staining kits (for charcoal nanoparticles). The fixed cells were stained with the Diff-Quik following the manufacturer's instruction (Dade Behring Inc, DE). Microscopic analysis was conducted on a Nikon E600 polarizing microscope equipped

with a Nikon DXM 1200 digital camera and filters for light polarization.

Intratracheally Instilled Nanoparticles

Male Sprague Dawley (SD) rats (~350–400 g) from Charles Rivers Labs were anesthetized with 4–5% Isoflurane anesthesia for oro-tracheal administration of 0.5% Tween 80 vehicle and nano-suspension (4 mg/rat). The rats were positioned to allow visualization of their vocal cords and trachea using an otoscope. A Hamilton syringe was used to inject 100 μL of pyrene nanosuspension directly into the trachea. At 30 min and 120 min after oro-tracheal dosing, rats were euthanized with 30 mg/kg pentobarbitol (Sleepaway) injection intraperitoneally. The throat was incised exposing the trachea and a cannula inserted for bronchoalveolar lavage (BAL). BAL fluid collection was performed through four instillations of 2.5 mL each, 10 mL in total. After each BAL was recovered, the fluid was placed in a 15 mL conical tube on ice. The BAL fluid was centrifuged at 900*g* for 15 min at 4 °C to precipitate the cells. After being placed on glass slides, the cells were fixed with 10% paraformaldehyde for 30 min and then stained with the Diff-Quik kit. A similar protocol was conducted for charcoal nanoparticles and was followed by the histopathological examination. The Pfizer Institutional Animal Care and Use Committee (IACUC) reviewed and approved the animal use in these studies. The Association for Assessment and Accreditation of Laboratory Animal Care, International fully accredits the Pfizer animal care and use program.

Histopathology

At necropsy, the entire lung pluck with trachea was removed. Lung lobes were instilled with approximately 10 mL of 10% neutral buffered formalin (NBF). The trachea was clamped with a bull dog style clip to retain instilled formalin throughout fixation. Lungs were fixed for 24 h in 10% NBF. Lung lobes were cassetted individually to maintain identity and processed whole on a Sakura VIP 5 series by dehydrating through a series of graded ethanol solutions, cleared with xylene and impregnated with paraffin. Lung lobes were embedded ventral aspect down in block. Sections of 4 μm thickness were cut to expose intrapulmonary airways for each lung lobe. Sectioned tissues were heated in a 60° oven for a minimum of 1 h, stained via automated linear stainer with hematoxylin–eosin and coverslipped. The processed glass slides were evaluated under Olympus light microscope and the images were captured by Spot Insight Firewire Camera and analyzed by Spotsoftware Advanced (Diagnostic Instruments, Inc., Sterling Heights, MI).

Results and Discussion

Wet Milling Preparation and the Solid State Properties of Nanoparticles

Particle size reduction can be achieved by pressure, friction, attrition impact, or shear. Milling technologies (wet or dry) are well-established and convenient techniques for size reduction [11]. Nanosuspensions are formed by building particles during precipitation or breaking, as in milling, and results in new formations that increase the total surface area. During the milling process, more free energy is generated and the system tends to agglomerate. However, this can be mitigated by the addition of surfactants. Surfactant provides a higher energy barrier to aggregation by changing the interaction of the surface of the primary particles. In some cases, electrostatic charges and amorphous domains on the particle surface induced by the milling process, render the ground material both cohesive and adhesive. These physical and chemical changes caused by size reduction are highly undesirable and can adversely affect the performance and improvement in drug absorption. Low solubility and high logP are recognized as two of the major challenges in the drug discovery. Therefore, pyrene, which represents the class of chemicals, was selected as a surrogate material to test for the purpose. In contrast, charcoal, the absolute non-soluble material resisting to the solvents during sample preparing, was picked for understanding the intrinsic behaviors of nano particles, and for the convenience of imaging as well. In this experiment, we used a bench scale wet milling device invented by Haskell [10], in which the materials in the presence of surface stabilizers are comminuted by milling media and the particle size reduction is determined by the shear intensity and the number of contact points. In our nanopreparations, the mean particle size for all materials fell in between 0.3 and 0.6 μm following the milling procedure; for pyrene, D25/D50/D90: 0.19/0.34/0.68 μm; for charcoal, D25/D50/D75:0.15/0.25/0.44. Furthermore, for the above reasons, the solid state properties of pyrene were monitored both pre- and post-milling using powder X-ray diffraction (PXRD). There were no obvious form changes in the post-milled material (Fig. 1a). The nanoparticle distribution in optical microscopy (Nikon E600 pol) was shown in Fig. 1b. The results imply that the wet milling process was an adequate technique for particle size reduction for these highly crystalline small molecules and should be highly relevant when considering drug particle stability in this system.

Nanoparticles Uptake in Epithelial Cell Lines

The oral bioavailability of a poorly absorbed molecule can be improved by size reduction to the nanoparticle range.

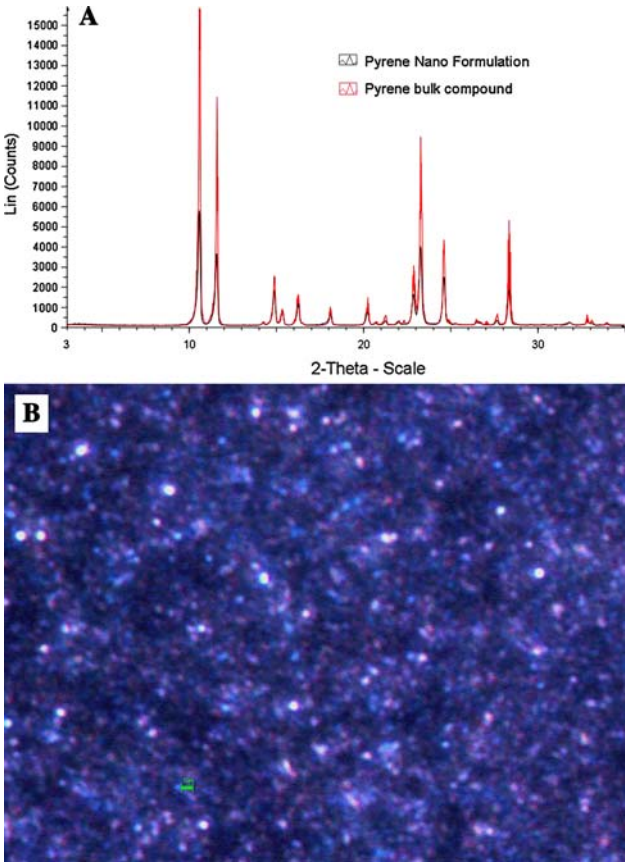

Fig. 1 (**a**) The solid state properties of pyrene were monitored at pre- and post-milling using powder X-ray diffraction (PXRD) in a Bruker D-8 Advance diffractometer. Data were collected using a step scan of 0.02° per point with a one second/point counting time over a range of 3°–35° two-theta. No changes of solid state properties of pyrene were observed. (**b**) Distribution of nano pyrene. The image was taken on a Nikon E600 polarizing microscope equipped with a Nikon DXM 1200 digital camera and filters for light polarization. Bar = 1 μm

Leroux et al. [12] have demonstrated significant improvement in bioavailability for HIV-1 protease inhibitors using pH sensitive nanoparticles, as the smaller particle size can increase surface area resulting in an increased dissolution rate and bioavailability. Transmucosal passage of microparticles from the intestinal lumen to the systemic circulation has been also observed [13]. In addition, by reducing the size of particles to the sub-micron level, enhanced uptake of intact polymeric particles was observed in pre-clinical experiments [14, 15]. However, the relevant importance and mechanism of directly cellular nanoparticles uptake in overall improvement of drug absorption or targeting delivery remains unclear.

The Caco-2 cell line, derived from human colorectal carcinoma, spontaneously differentiates in culture to form confluent monolayers with remarkable morphological and biochemical similarity to the small intestinal epithelium [16]. Caco-2 cells have been developed as a useful alternative to animal models to study intestinal absorption of therapeutic agents including proteins, peptides, and oligonucleotides, showing promise that might give useful predictions concerning the oral absorption potential [17–19]. Therefore, the nanoparticles uptake studies observed in Caco-2 cells could probably be considered to correlate with in vivo situations. As shown in Fig. 2, both of charcoal and pyrene nanoparticles were found in the cytoplasm of the Caco-2 cells, though the nanoparticles in cytoplasm of the Caco-2 cells were scattered (2–4 particles per scene) up to a 4 h incubation period. The results suggest that the uptake of intact nanoparticle by Caco-2 cells was limited. This correlates with previously reported in vivo results that the contribution of nanoparticles uptake on bioavailability improvement of small molecules is limited, and the percentage of nanoparticles absorbed via the nanoparticles transcytosis mechanism in the administrated dose is varied ranged from 0.01 to 3.6% [6, 14, 20]. In contrast to our observations, significantly greater tissue uptake for biodegradable nanoparticles, such as polylactic-polyglycolic acid co-polymer nanoparticles and lectin-coated nanoparticles, have been observed. This variation in uptake has important implications for designing nanoparticle-based oral drug delivery systems, such as an oral vaccine system [21–23]. Different from the crystallized small molecule in absorption, these biodegradable particles, such as lectins and invasins, can bind to the intestinal epithelial cells and stimulate the uptake and transport of nanoparticles [9, 24–26], suggesting the existence of carrier mediated transport in intestinal epithelial cells or Caco-2 cells. Therefore, a size-dependent transcytosis transport of biodegradable particles in the gastrointestinal mucosal tissue might not be

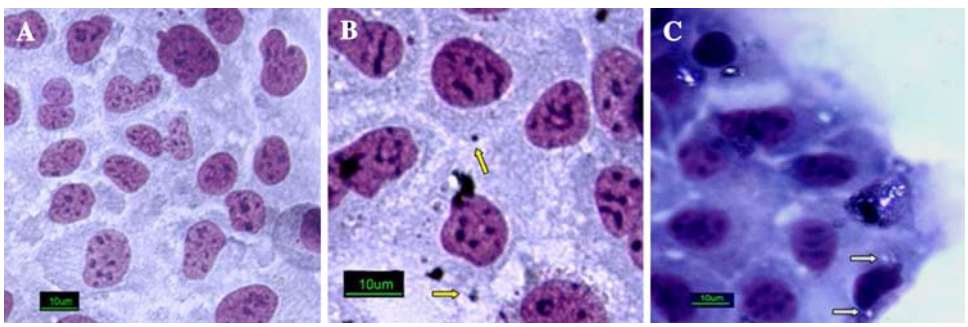

Fig. 2 Nanoparticle uptake in Caco-2 cells. The pyrene or charcoal was applied in a separated set of cells. (**a**) control cells; (**b**) Caco-2 cell incubated with charcoal nanoparticles for 4 h; (**c**) Caco-2 cells incubated with pyrene nanoparticles for 4 h

translatable to crystallized small molecules for the lack of the nanoparticle carriers. In this study, the limited uptake of nanoparticles in Caco-2 cells suggested that the transcytosis transport of nanoparticles of small molecule directly into systemic circulation might be not considered as a major factor contributing to the improvement of drug bioavailability. The fact that limited direct uptake of nanoparticle in Caco-2 cells suggested that the improvement of oral bioavailability [27] by the particle size reduction is via increased dissolution rate rather than direct uptake.

Recently, Madin-Darby Canine Kidney (MDCK) cells have been an alternate model to Caco-2 cells for permeability screening [28]. Similar to Caco-2 cells, MDCK cells differentiate into columnar epithelium and form tight junctions when cultured on semi-permeable membranes. Primarily for passively absorbed compounds, the permeability obtained from MDCK assays have been shown to be similar to that from Caco-2 assays [29]. MDCK cells, like the intact brain–blood barriers (BBB) (but unlike most in vitro endothelial cell models), also have a transmembrane resistance but much lower than that in Caco-2 cells, and thus the model is more relevant to assess passive diffusion across the BBB. In a recent comprehensive comparison of numerous in vitro models, MDCK cells have been considered to offer the best model in terms of predicting BBB penetration based on microdialysis data [30]. When incubated with MDCK cells, nanoparticles were found traversing though the cell membrane after 2 h incubation. After 4 h incubation, the majority of nanoparticles were located in the perinuclear region of the cells. The nanoparticles entered the cells and were trapped inside the cytoplasm but did not appear in the cell nucleus (Fig. 3b). A greater extent of nanoparticle engulfment was observed compared to that in Caco-2 cells. The results suggested that significant difference exists in nanoparticle uptake among the different cell lines, which might reflect the difference in translocation of nanoparticles in vivo.

We know that ATP binding cassette (ABC) transporters are present in virtually every cell and they play a central role in physiology. They may be pivotal in the protection of against xenobiotics entering the organs or cells [31]. Moreover, multiple efflux transporters are identified in Caco-2 cell and intestinal epithelial cells, and are responsible for restricting intestine absorptions for their substrates [32]. However, the effects of efflux transporter(s) on nanoparticle uptake remain unknown. Recently, MDCK cells genetically modified to overexpress human P-glycoprotein (P-gp) have been shown to effectively discriminate compounds that cross the BBB but are not P-gp substrates from those that cross the BBB but are P-gp substrates. This, along with the ability to assess P-gp transport, makes them a very useful in vitro tool to assess the BBB permeation of compounds and the extent of outwardly directed active efflux [30]. In addition, the delivery of pulmonary drugs to the site of action may also depend on the presence and activity of many ABC transporters [33]. Even though there is no direct evidence showing that efflux transporters might prevent nanoparticles uptake from the cells, it would be of further interest to investigate if the efflux mechanism on the cells barriers (e.g. BBB or chemotherapy) could be bypassed by using nanoparticles as a carrier system to enhance uptake of the agents which are otherwise poorly deposited because of the transporter mediated efflux [34]. To test the hypothesis, a similar experiment protocol was applied to a MDCK-MDR1 cell that was genetically engineered to overexpress P-gp. Not surprisingly, a similar pattern of nanoparticle uptake was found in both the MDCK and MDCK-MDR1 cells (Fig. 3). Significant MDCK and MDCK-MDR1 cell engulfment of nanoparticles suggested that nanoformulation might be a useful tool to overcome the BBB and/or efflux transporters in chemotherapy via transcytosis mechanism.

Nanoparticles Uptake in Mouse Macrophage Cells

Despite the low percentage of uptake for orally administrated doses in GI tract, Clark et al. [35] reported that M-cells in Peyer's patches of the gastrointestinal lymphoid tissues are involved the mechanisms in particulate pathway of gastrointestinal absorption. Macrophage uptake, e.g. Kuffer cells in liver, has also been reported to involve the distribution of intravenously administered nanoparticles [36]. To examine the nanoparticles uptake in monocytes,

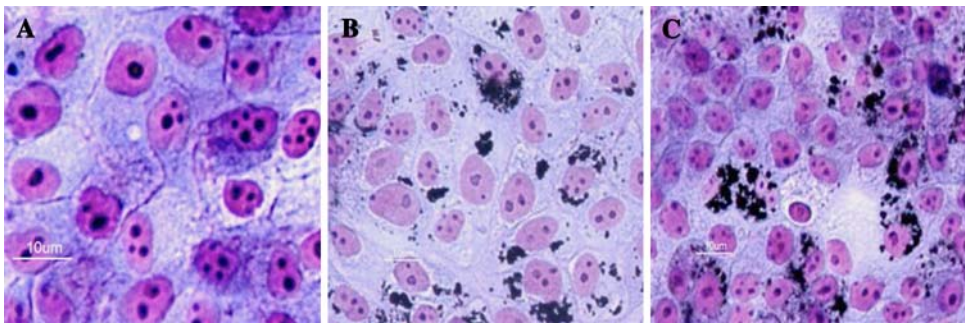

Fig. 3 Uptake of Charcoal nanoparticles in MDCK and MDCK-MDR1 cells. (**a**) MDCK cell; (**b**) MDCK cells incubated with nanoparticles for 4 h; (**c**) MDCK-MDR1 cells incubated with nanoparticle for 4 h

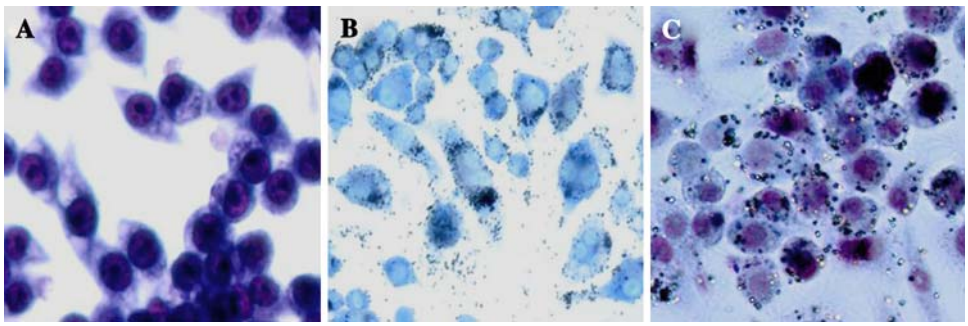

Fig. 4 Nanoparticle uptake in RAW cells: (**a**) control cell; (**b**) incubation with charcoal particles for 4 h; (**c**) incubation with pyrene particles for 4 h

nanoparticles of pyrene and charcoal were incubated with mouse macrophage RAW cells. Nanoparticles uptake by RAW cell over 4 h time period was monitored by light microscopy. These cells extensively took up the administered nanoparticles through non-specific transcytosis. As shown in Fig. 5, large amounts of nanoparticles were engulfed into the cytoplasm of the RAW cells. Among the cell lines tested, RAW cells had the greatest capability for nanoparticles uptake for both pyrene (Fig. 4b) and charcoal (Fig. 4c) among the cell lines tested. Our results indicated that the extent of nanoparticles uptake into cells is dependent upon the cell type and origin. These results not only show that there are differences in nanoparticles uptake in various cellular matrix, but also indicated that these significant differences in in vitro cell lines should be taken into consideration and integrated into the design of nanoparticle formulation development.

Pulmonary Cellular Uptake of Nanoparticles in Intratracheally Dosed Rat Model

Particle size and morphology have a pronounced effect on all aspect of drug delivery to the lungs. Research has shown that particles below 5 μm can be distributed deeply into the

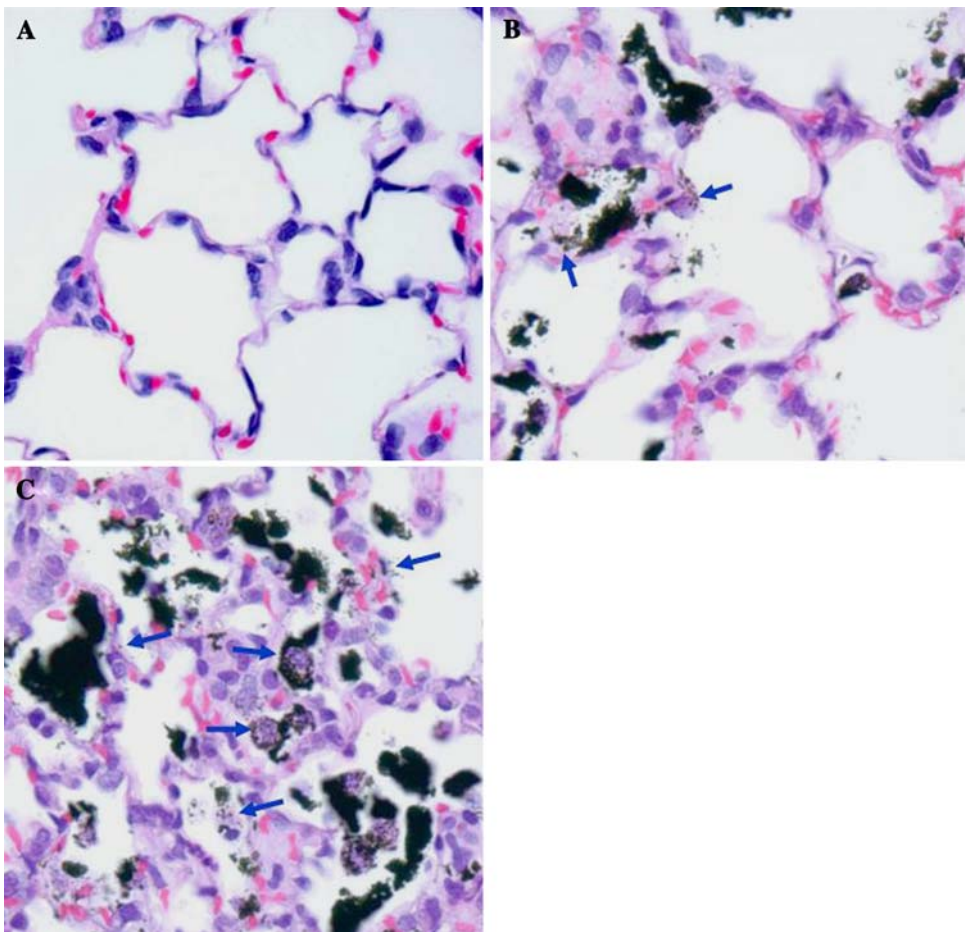

Fig. 5 Histopathological images of nanoparticle inhaled rat model (20×). (**a**) Normal terminal bronchi and alveoli structures; (**b**) At 30 min post-IT injections, the charcoal particles attached to and/or absorbed (arrow heads) by the bronchial epithelium, alveolar epithelium and residual macrophages; (**c**) At 120 min post-IT injections, the charcoal particles distributed in cytoplasm of macrophages, type II alveolar epithelial cells and bronchial epithelial cells (arrow heads). The alveolar type I epithelial cells are cuboidal and hyperplastic. Most of the type II alveolar cells had numerous intracytoplasmic nanoparticles and hypertophic

smaller airways, delaying the effect on phagocytic clearance which can lead to longer action time [37]. Nemmar et al. [5] reported that untrafine technetium (99mTC) labeled carbon particles diffused, within 5 min, into the systemic circulation, and concluded that in addition to the particle translocation to the blood via phagocytosis by macrophages and/or endocytosis by epithelial and endothelial cells, other pathway(s) must also exist. We hypothesize that direct transport of intact nanoparticles through epithelial cell layers might also attribute to translocation of inhaled particles into the systemic circulation. In our study, an intratracheal nanoparticles dosed rat model was used to investigate nanoparticles translocation across lung epithelial cells and nanoparticle phagocytosis in BAL fluid cells. For ease of detection and preventing the loss of particle appearance during sample preparation, charcoal nanoparticles were used in the rats for histopathological sections. Post-necropsy, thin sections of lung were stained with hematoxylin–eosin and then examined by light microscopy. At 30 min and 2 h post-intratracheally injection, the lining tracheal epithelial cells of trachea, bronchi, and bronchioli had various amount of the charcoal particles deposited (Fig. 5b, c). Most deposited nanoparticles were located at the terminal bronchioles and the surrounding alveoli. Different from the epithelial surface retention observed for micron-sized poly-styrene and glass particles [38, 39], the alveolar cells and the alveolar macrophages had charcoal particles on the surface as well as in the cytoplasm (Fig. 5b). The deposits of charcoal particles on the surface and intracytoplasm of endothelial cells and type I epithelial cells (Fig. 5) were not obvious. At 30 min post-injection, there were no morphological changes of the alveolar epithelial cells and no evidence of inflammatory infiltrations (Fig. 5b). However, at 2 h post-intratracheal injection of nanoparticles, there were minimum infiltrations of neutrophils. The alveolar epithelial cells, most likely type II cells at the terminal bronchioles and its surrounding alveoli became cuboidal, an indication of early cellular activation (Fig. 5c). Our results reconfirmed with a number of morphologic studies showing that nanoparticles penetrated into and beyond the epithelium rather rapidly. For instance, uptake of nanoparticles in type I epithelial cells, endothelial cells, and the alveolar septum of ultrafine gold-particles was recently confirmed by transmission electron

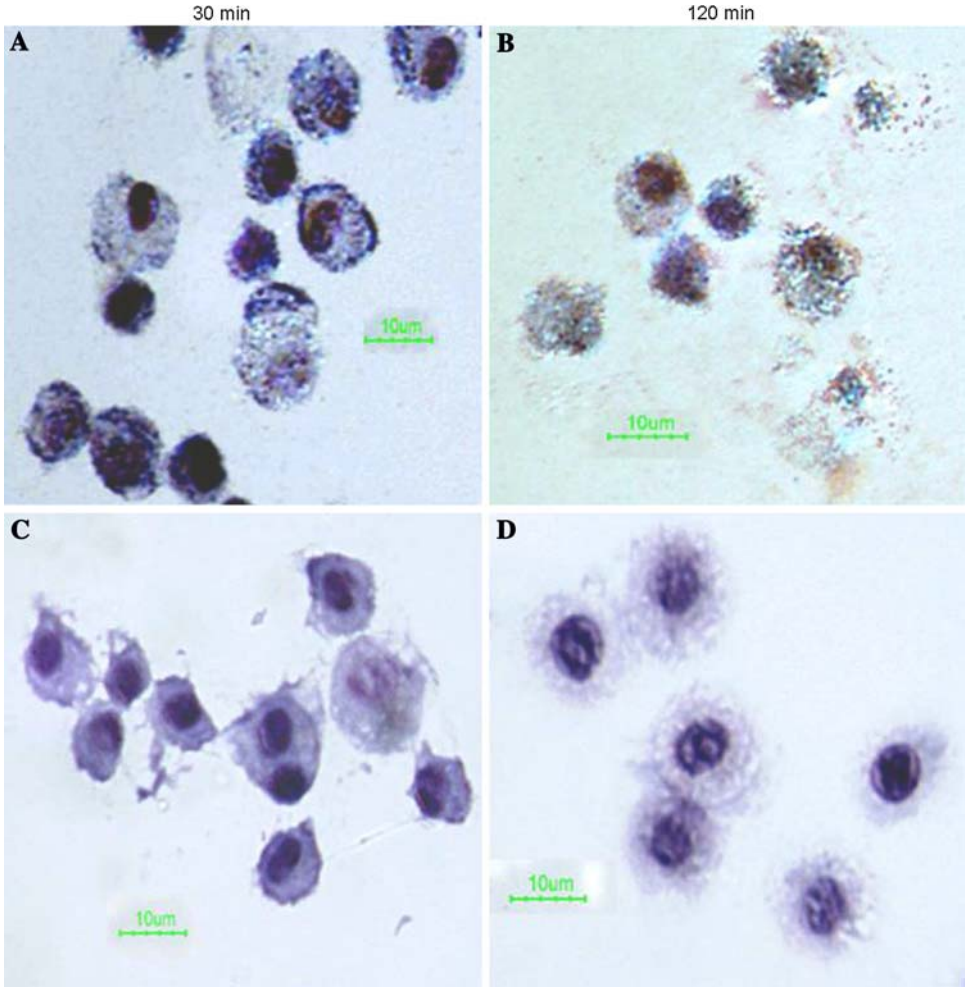

Fig. 6 Nanoparticle uptake in cell from BAL fluid: (**a**) the uptakes of nanoparticle in BAL cells at 30 min post-IT injection, (**b**) the uptake of nanoparticles in BAL cells at 120 min post-IT injection. (**c**, **d**) BAL cells in control group at 30 min and 120 min post-IT injections, respectively

microscopy [40]. In addition, Castranova et al. has reported the evidences for uptake of ultrafine particles (nanoparticles) in epithelial cells and in the interstitial spaces, translocation into systemic circulation, and accumulation in secondary target organs [41]. As mentioned above, we administrated the water-insoluble charcoal nanoparticle; therefore, the morphological change might be in agreement with adaptive pulmonary responses to water non-soluble charcoal nanoparticle. In fact, the significant uptake of inhaled nanoparticles were detected in the cells from BAL fluids (Fig. 6) as early as 30 min post-intratracheal injection of nanoparticles, and the damages in BAL cells were also observed at 2 h post-dosing (Fig. 6). These early responses might be the initial indications of granulomatous reactions observed at the late stage [42]. This morphology indicated that the intratracheal delivery of absolute water non-soluble nanoparticles, at least in our case, may be the cause of pulmonary granulomatous reaction at late stage. However, this reaction should be considered to be independent of the active drug components. Therefore, the success of nanoformulation would probably depend on chemophysiological properties of nanoparticles and toxicological issues associated with understanding of the fate of nanoparticles in vivo. The chronic implications of the early inflammatory responses to the nanoparticles warrant further investigation.

In conclusion, while the uptake of small molecule, crystalline nanoparticles in caco-2 cells, which represents a GI absorption model, was limited, a greater uptake was observed in MDCK and MDCK cells overexpressing P-gp. In addition, extensive uptake was observed in mouse macrophage-like RAW cell, suggesting that nanoparticle uptake is highly dependent on the cell type. The improvement of oral bioavailability by particle size reduction is via increased dissolution rate rather than direct uptake; however, the approach of nanoparticle delivery might further improve efficacy and practicability of inhaled delivery and/or to overcome efflux transporter barriers in chemotherapy or CNS delivery.

Acknowledgment We would like to thank Drs. Timothy G Heath and Joeseph Fleishaker for their helpful comments and suggestions on our study.

References

1. B.E. Rabinow, Nat. Rev. Drug Discov. **3**, 785–796 (2004). doi:10.1038/nrd1494
2. J. Jinno, N. Kamada, M. Miyake, K. Yamada, T. Mukai, M. Odomi et al., J. Control Release **111**, 56–64 (2006). doi:10.1016/j.jconrel.2005.11.013
3. J. Kreuter, Eur. J. Drug Metab. Pharmacokinet. **19**, 253–256 (1994)
4. P. Kocbek, S. Baumgartner, J. Kristl, Int. J. Pharm. **312**, 179–186 (2006). doi:10.1016/j.ijpharm.2006.01.008
5. A. Nemmar, H. Vanbilloen, M.F. Hoylaerts, P.H. Hoet, A. Verbruggen, B. Nemery, Am. J. Respir. Crit. Care Med. **164**, 1665–1668 (2001)
6. M. Doyle-McCullough, S.H. Smyth, S.M. Moyes, K.E. Carr, Int. J. Pharm. **335**, 79–89 (2007). doi:10.1016/j.ijpharm.2006.10.043
7. M. Huang, Z. Ma, E. Khor, L.Y. Lim, Pharm. Res. **19**, 1488–1494 (2002). doi:10.1023/A:1020404615898
8. R. Ghirardelli, F. Bonasoro, C. Porta, D. Cremaschi, Biochim. Biophys. Acta. **1416**, 39–47 (1999). doi:10.1016/S0005-2736(98)00209-0
9. G.J. Russell-Jones, H. Veitch, L. Arthur, Int. J. Pharm. **190**, 165–174 (1999). doi:10.1016/S0378-5173(99)00254-9
10. Haskell RJ, Laboratory scale milling process, U.S. Patent, Pharmacia & Upjohn Company, US, 2004
11. E. Merisko-Liversidge, G.G. Liversidge, E.R. Cooper, Eur. J. Pharm. Sci. **18**, 113–120 (2003). doi:10.1016/S0928-0987(02)00251-8
12. J.C. Leroux, R.M. Cozens, J.L. Roesel, B. Galli, E. Doelker, R. Gurny, Pharm. Res. **13**, 485–487 (1996). doi:10.1023/A:1016073416332
13. M. Aprahamian, C. Michel, W. Humbert, J.P. Devissaguet, C. Damge, Biol. Cell **61**, 69–76 (1987)
14. P. Jani, G.W. Halbert, J. Langridge, A.T. Florence, J. Pharm. Pharmacol. **42**, 821–826 (1990)
15. A.T. Florence, N. Hussain, Adv. Drug Deliv. Rev. **50**(Suppl 1), S69–S89 (2001). doi:10.1016/S0169-409X(01)00184-3
16. I.J. Hidalgo, T.J. Raub, R.T. Borchardt, Gastroenterology **96**, 736–749 (1989)
17. I. Behrens, P. Stenberg, P. Artursson, T. Kissel, Pharm. Res. **18**, 1138–1145 (2001). doi:10.1023/A:1010974909998
18. J. Taipalensuu, H. Tornblom, G. Lindberg, C. Einarsson, F. Sjoqvist, H. Melhus et al., J. Pharmacol. Exp. Ther. **299**, 164–170 (2001)
19. A.M. Calcagno, J.A. Ludwig, J.M. Fostel, M.M. Gottesman, S.V. Ambudkar, Mol. Pharm. **3**, 87–93 (2006). doi:10.1021/mp050090k
20. J.P. Ebel, Pharm. Res. **7**, 848–851 (1990). doi:10.1023/A:1015964916486
21. L. Zhang, M. Sun, R. Guo, Z. Jiang, Y. Liu, X. Jiang et al., J. Nanosci. Nanotechnol. **6**, 2912–2920 (2006). doi:10.1166/jnn.2006.431
22. M.P. Desai, V. Labhasetwar, G.L. Amidon, R.J. Levy, Pharm. Res. **13**, 1838–1845 (1996). doi:10.1023/A:1016085108889
23. M.P. Desai, V. Labhasetwar, E. Walter, R.J. Levy, G.L. Amidon, Pharm. Res. **14**, 1568–1573 (1997). doi:10.1023/A:1012126301290
24. W. Easson, Vet. Rec. **140**, 636 (1997)
25. G.J. Russell-Jones, L. Arthur, H. Walker, Int. J. Pharm. **179**, 247–255 (1999). doi:10.1016/S0378-5173(98)00394-9
26. N. Hussain, P.U. Jani, A.T. Florence, Pharm. Res. **14**, 613–618 (1997). doi:10.1023/A:1012153011884
27. L. Jia, H. Wong, C. Cerna, S.D. Weitman, Pharm. Res. **19**, 1091–1096 (2002). doi:10.1023/A:1019829622088
28. J.D. Irvine, L. Takahashi, K. Lockhart, J. Cheong, J.W. Tolan, H.E. Selick et al., J. Pharm. Sci. **88**, 28–33 (1999). doi:10.1021/js9803205
29. W.S. Putnam, L. Pan, K. Tsutsui, L. Takahashi, L.Z. Benet, Pharm. Res. **19**, 27–33 (2002). doi:10.1023/A:1013647114152
30. P. Garberg, M. Ball, N. Borg, R. Cecchelli, L. Fenart, R.D. Hurst et al., Toxicol. In Vitro **19**, 299–334 (2005). doi:10.1016/j.tiv.2004.06.011
31. G.L. Scheffer, A.C. Pijnenborg, E.F. Smit, M. Muller, D.S. Postma, W. Timens et al., J. Clin. Pathol. **55**, 332–339 (2002)

32. V.D. Makhey, A. Guo, D.A. Norris, P. Hu, J. Yan, P.J. Sinko, Pharm. Res. **15**, 1160–1167 (1998). doi:10.1023/A:1011971303880
33. K.O. Hamilton, M.A. Yazdanian, K.L. Audus, Curr. Drug Metab. **3**, 1–12 (2002). doi:10.2174/1389200023338170
34. I.J. Hidalgo, Pharm. Biotechnol. **8**, 35–50 (1996)
35. M.A. Clark, M.A. Jepson, B.H. Hirst, Adv. Drug Deliv. Rev. **50**, 81–106 (2001). doi:10.1016/S0169-409X(01)00149-1
36. S.M. Moghimi, A.C. Hunter, J.C. Murray, Pharmacol. Rev. **53**, 283–318 (2001)
37. A.H. Chow, H.H. Tong, P. Chattopadhyay, B.Y. Shekunov, Pharm. Res. **24**, 411–437 (2007). doi:10.1007/s11095-006-9174-3
38. B.E. Lehnert, Y.E. Valdez, G.L. Tietjen, Am. J. Respir. Cell Mol. Biol. **1**, 145–154 (1989)
39. G. Oberdorster, J. Ferin, B.E. Lehnert, Environ. Health Perspect. **102**(Suppl 5), 173–179 (1994). doi:10.2307/3432080
40. S. Takenaka, E. Karg, W.G. Kreyling, B. Lentner, W. Moller, M. Behnke-Semmler et al., Inhal. Toxicol. **18**, 733–740 (2006). doi:10.1080/08958370600748281
41. M. Geiser, B. Rothen-Rutishauser, N. Kapp, S. Schurch, W. Kreyling, H. Schulz et al., Environ. Health Perspect. **113**, 1555–1560 (2005)
42. V. Castranova, D. Porter, L. Millecchia, J.Y. Ma, A.F. Hubbs, A. Teass, Mol. Cell Biochem. **234–235**, 177–184 (2002). doi:10.1023/A:1015967017103